

# The structure of $\kappa/\iota$ -hybrid carrageenans II. Coil–helix transition as a function of chain composition<sup>☆</sup>

Fred van de Velde,<sup>a,b,\*</sup> Anna S. Antipova,<sup>a</sup> Harry S. Rollema,<sup>b</sup> Tatiana V. Burova,<sup>c</sup> Nataliya V. Grinberg,<sup>c</sup> Leonel Pereira,<sup>d</sup> Paula M. Gilseman,<sup>e</sup> R. Hans Tromp,<sup>a,b</sup> Brian Rudolph<sup>e</sup> and Valerij Ya. Grinberg<sup>c</sup>

<sup>a</sup>Wageningen Centre for Food Sciences, PO Box 557, 6700 AN Wageningen, The Netherlands

<sup>b</sup>NIZO Food Research, Texture Department, Kernhemseweg 2, PO Box 20, 6710 BA Ede, The Netherlands

<sup>c</sup>Institute of Biochemical Physics, Russian Academy of Sciences, 119991 Moscow GSP-1, Vavilov St. 28, Russian Federation

<sup>d</sup>University of Coimbra, Department of Botany, Arcos do Jardim, 3000 Coimbra, Portugal

<sup>e</sup>CP Kelco Aps, 4623 Lille Skensved, Denmark

Received 1 November 2004; accepted 14 February 2005

**Abstract**—This paper describes the effect of the  $\kappa/\iota$ -ratio on the physical properties of  $\kappa/\iota$ -hybrid carrageenans (synonyms: kappa-2,  $\kappa$ -2, weak kappa, weak gelling kappa). To this end, a series of  $\kappa/\iota$ -hybrid carrageenans ranging from almost homopolymeric  $\kappa$ -carrageenan (98 mol-%  $\kappa$ -units) to almost homopolymeric-carrageenan (99 mol-%  $\iota$ -units) have been extracted from selected species of marine red algae (Rhodophyta). The  $\kappa/\iota$ -ratio of these  $\kappa/\iota$ -hybrids was determined by NMR spectroscopy. Their rheological properties were determined by small deformation oscillatory rheology. The gel strength (storage modulus,  $G'$ ) of the  $\kappa/\iota$ -hybrids decreases with decreasing  $\kappa$ -content. On the other hand, the gelation temperature of the  $\kappa$ -rich  $\kappa/\iota$ -hybrids is independent of their composition. This allows one to control the gel strength independent of the gelation or melting temperature.

The conformational order–disorder transition of the  $\kappa/\iota$ -hybrids was studied using optical rotation and high-sensitivity differential scanning calorimetry. High-sensitivity DSC showed that the total transition enthalpy of the  $\kappa/\iota$ -hybrids goes through a minimum at 60 mol-%  $\kappa$ -units, whereas for the mixture of  $\kappa$ - and  $\iota$ -carrageenan, the total transition enthalpy is a linear function of the composition. With respect to the ordering capability, the  $\kappa/\iota$ -hybrid carrageenans seem to behave as random block copolymers with length sequence distributions truncated from the side of the small lengths. Intrinsic thermodynamic properties (e.g., transition temperature and enthalpy) of  $\kappa$ - and  $\iota$ -sequences in these copolymers are close to those of their parent homopolymers. The critical sequence length for  $\kappa$ -sequences is 2-fold of that for  $\iota$ -sequences.

© 2005 Elsevier Ltd. All rights reserved.

**Keywords:** Carrageenan;  $\kappa/\iota$ -Hybrids; Kappa-2; Polysaccharides; Coil-to-helix transition; Structural analysis; Differential scanning calorimetry

## 1. Introduction

Carrageenans represent one of the major texturising ingredients in the food industry. They are natural ingredients used for decades in food applications and are regarded as safe.<sup>2</sup> The dairy sector accounts for a large

part of the carrageenan applications in food products, such as frozen desserts, chocolate milk, cottage cheese and whipped cream.<sup>2–4</sup> In general, carrageenan serves as a gelling, stabilising and viscosity-building agent. Carrageenan is the generic name for a family of polysaccharides, obtained by extraction from certain species of red algae (Rhodophyta). They are mixtures of water-soluble, linear, sulfated galactans. They are composed of alternating 3-linked  $\beta$ -D-galactopyranose (G-units) and 4-linked  $\alpha$ -D-galactopyranose (D-units) or 4-linked 3,6-anhydrogalactose (DA-units), forming the ‘ideal’

<sup>☆</sup>This publication is part of a series on the properties of  $\kappa/\iota$ -hybrid carrageenans starting with Ref. 1.

\* Corresponding author. Tel.: +31 318 659 582; fax: +31 318 650 400; e-mail: [fred.van.de.velde@nizo.nl](mailto:fred.van.de.velde@nizo.nl)

disaccharide repeating unit of carrageenans (see Fig. 1). These sulfated galactans are classified according to the presence of the 3,6-anhydrogalactose on the 4-linked residue and the position and number of sulfate groups. The most common types of carrageenan are traditionally identified by a Greek prefix. The three commercially most important carrageenans are called  $\kappa$ -,  $\iota$ - and  $\lambda$ -carrageenan. In addition, two other types, called  $\mu$ - and  $\nu$ -carrageenan, are often encountered in carrageenan samples obtained by mild extraction methods. The  $\mu$ - and  $\nu$ -carrageenans are the biological precursors of, respectively,  $\kappa$ - and  $\iota$ -carrageenan. The  $\kappa$ - and  $\iota$ -carrageenans are gel-forming carrageenans, whereas  $\lambda$ -carrageenan is a thickener/viscosity builder. In general terms,  $\kappa$ -carrageenan gels are hard, strong and brittle, whereas  $\iota$ -carrageenan forms soft and weak gels that are shear reversible.<sup>2</sup> To describe more complex structures, a letter code based nomenclature for red algae galactans has been developed.<sup>5</sup> The letter codes for  $\kappa$ - and  $\iota$ -carrageenan are included in Figure 1.

The different types of carrageenan are obtained from different species of the Rhodophyta.  $\kappa$ -Carrageenan is predominantly obtained by extraction of the tropical seaweed, *Kappaphycus alvarezii*, known in the trade as *Eucheuma cottonii* (or simply Cottonii).<sup>6</sup> *Eucheuma denticulatum* (trade name *Eucheuma spinosum* or simply Spinosum) is the main species for the production of  $\iota$ -carrageenan. The largest commercial source of these tropical species is the Philippines where wild harvesting has been replaced by seaweed farming. The seaweeds are usually extracted with alkali at elevated temperatures to transform the biological precursors,  $\mu$ - and  $\nu$ -carrageenan, into  $\kappa$ - and  $\iota$ -carrageenans.  $\kappa/\iota$ -Hybrid carrageenans (synonyms: kappa-2,  $\kappa$ -2, weak kappa, weak gelling kappa) are obtained from different species in the Gigartinales family. The gametophytic thalli pro-

duce  $\kappa/\iota$ -hybrid carrageenans, whereas the sporophytic thalli of these seaweeds produce  $\lambda$ -carrageenan and other related carrageenan types, such as  $\xi$ ,  $\theta$  and  $\pi$ -carrageenan.<sup>7,8</sup>

The structure of the  $\kappa/\iota$ -hybrid carrageenans has been a major topic for several research groups. Several schemes are conceivable for these  $\kappa/\iota$ -hybrids: a mixture of homopolymeric  $\kappa$ - and  $\iota$ -carrageenan chains or a mixed or heteropolymeric chain comprising both  $\kappa$ - and  $\iota$ -repeating units. In the later case, the distribution can be either blockwise or random. Small amounts of  $\iota$ -carrageenan present in *K. alvarezii* extracts are identified to be separated chains.<sup>9</sup> However,  $\kappa/\iota$ -hybrids with a more equal distribution of  $\kappa$ - and  $\iota$ -repeating units are found to be heteropolymeric type of  $\kappa/\iota$ -hybrids.<sup>1,10,11</sup> From an industrial point of view, the  $\kappa/\iota$ -hybrids are of increasing importance for their specific functionalities in dairy applications.<sup>8,11,12</sup> The term kappa-2 carrageenan has been arbitrarily given to  $\kappa/\iota$ -hybrid carrageenans with a  $\kappa$ -content from 80 to 45 mol-%  $\kappa$ -repeating units.<sup>10,12</sup> Within this study the term  $\kappa/\iota$ -hybrid carrageenan is preferred as the samples range from homopolymeric  $\kappa$ -carrageenan to homopolymeric  $\iota$ -carrageenan. The different algal sources producing these  $\kappa/\iota$ -hybrids are generally summarised in a so-called Stancioff diagram<sup>10,13</sup> (see also Fig. 3). The original, commercial source of the  $\kappa/\iota$ -hybrid carrageenan was *Chondrus crispus* (from Canada), also known as Irish moss. At present, *Sarcothalia crispata*, *Gigartina skottsbergii* and *Chondracanthus chamissoi* (from Chile), known in trade as Luga Negra, Gigartina broad leaf or simply Gigartina are the important species for the commercial production of this carrageenan. The harvesting from natural populations has been and will be restricted by several authorities and, thereby, stimulating the research in seaweed production by aquaculture.<sup>8,14,15</sup> For this reason several red seaweed species were analysed for the presence of  $\kappa/\iota$ -hybrid carrageenans in relation to their functional properties. Moreover, a vast amount of literature is available on the analysis of specific carrageenans produced by the different life stages of species belonging to Gigartinales. The list of studied species includes *C. crispus*, *Gigartina alveata*, *G. clavifera*, *G. decipiens*, *G. pistillata*, *G. skottsbergii*, *Gymnogongrus torulosus*, *S. crispata*, *S. atropurpurea* and several commercial and underutilised species collected from the occidental Portuguese coast.<sup>8,10–12,16–24</sup>

Although the functional properties in dairy applications have been studied for  $\kappa/\iota$ -hybrids extracted from specific species, no systematic analysis of the  $\kappa/\iota$ -hybrids has been reported. Most of the studies mentioned above started from a certain seaweed species and studied the functional properties of the carrageenans extracted. In contrast, we focus on the physical properties of the  $\kappa/\iota$ -hybrids, whereby the botanical source is of secondary importance. We focused on purified  $\kappa/\iota$ -hybrid

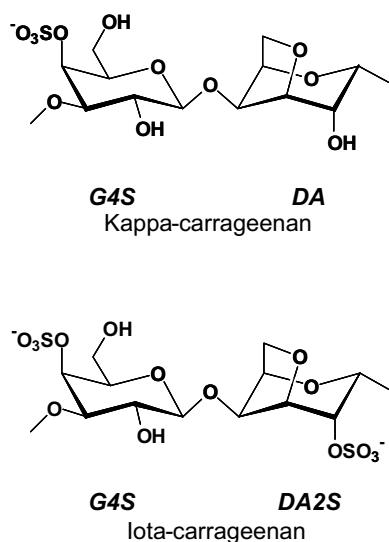


Figure 1. Molecular structure of carrageenan repeating units.

carrageenans, without additional carrageenan repeating units or contaminants, such as floridean starch or pyruvate acetal side chains, disturbing their molecular structure. Therefore, we investigated the effect of the  $\kappa/\iota$ -ratio of these  $\kappa/\iota$ -hybrids on their physical properties. To this end, we collected a series of  $\kappa/\iota$ -hybrid carrageenans, ranging from homopolymeric  $\kappa$ -carrageenan (98 mol-%) to homopolymeric  $\iota$ -carrageenan (99 mol-%), extracted from a wide variety of red algal species.  $^1\text{H}$  NMR spectroscopy was used as the preferred analytical technique to determine the molecular ratio of  $\kappa$ - and  $\iota$ -repeating units.<sup>25</sup> The coil-to-helix transition of the samples was studied by optical rotation measurements and high-sensitivity differential scanning calorimetry (HSDSC). Their rheological behaviour was determined by small deformation oscillatory measurements.

## 2. Experimental

### 2.1. Materials

Alkaline-extracted carrageenan samples were obtained from CP Kelco (Lille Skensved, Denmark), Degussa Texturant Systems (former SKW Biosystems, Boulogne, Billancourt Cedex, France) or the University of Coimbra (Coimbra, Portugal). Carrageenan samples used in this study are listed in Table 1.  $\alpha$ -Amylase from porcine pancreas was purchased from Aldrich–Sigma Chemie (Zwijndrecht, the Netherlands). All other salts and chemicals were of analytical grade.

### 2.2. Sample treatment

Samples containing floridean starch were treated with  $\alpha$ -amylase prior to alkaline treatment. Carrageenan (0.5% wt/wt; 1 g) was dissolved in reversed osmosis (RO) water at 85 °C and cooled to 30 °C. The pH was adjusted to 7.0 with concentrated HOAc. Porcine pancreas  $\alpha$ -amylase (100  $\mu\text{L}$ ) was added, and the mixture was incubated for 16 h at 30 °C. Subsequently, an alkaline treatment was carried out to hydrolyse the protein (see next paragraph).

Samples containing precursor units ( $\nu$ - or  $\mu$ -carrageenan) were treated with hot alkaline solution. Either carrageenan (0.5% wt/wt) was dissolved in RO-water at 85 °C or the  $\alpha$ -amylase-treated solution was used. A concentrated NaOH solution was added to a final concentration of 0.25 M. The solution was heated under reflux for 3 h.

All samples were dialysed against NaCl solution to obtain the  $\kappa/\iota$ -hybrid carrageenans in the pure Na-form. Either carrageenan (0.5% wt/wt) was dissolved in RO-water at 85 °C or the previously prepared solutions were used. While hot, EDTA (50 mM) was added to the carrageenan solutions to ensure the removal of divalent

metal ions. Solutions (200 mL) were dialysed against sodium chloride (0.1 M NaCl containing 20 mM  $\text{Na}_2\text{HPO}_4$ ;  $2 \times 2$  L), phosphate buffer (20 mM  $\text{Na}_2\text{HPO}_4$ ;  $3 \times 2$  L), water ( $1 \times 2$  L) and lyophilised.

### 2.3. NMR spectroscopy

The ratio between  $\kappa$ - and  $\iota$ -repeating units was determined by  $^1\text{H}$  NMR spectroscopy.  $^1\text{H}$  NMR spectra were recorded at 65 °C on a Bruker DRX 500 spectrometer operating at 500.13 MHz. Typically 64 scans were taken with an interpulse delay of 20 s ( $T_1$  values for the resonances of the anomeric protons of  $\kappa$ - and  $\iota$ -carrageenan are shorter than 1.5 s). Sample preparation for the  $^1\text{H}$  NMR experiments involved dissolving the carrageenan sample (5 mg  $\text{mL}^{-1}$ ) at 80 °C in  $\text{D}_2\text{O}$  containing 1 mM TSP (3-(trimethylsilyl)propionic-2,2,3,3- $d_4$  acid sodium salt), followed by sonication for  $3 \times 1$  h in a sonicator bath (Branson 2510).

$^{13}\text{C}$  NMR spectra were taken on a Bruker DRX 500 spectrometer operating at 125.76 MHz essentially as described in the literature.<sup>25,26</sup> The sample preparation was as follows. A solution of 5 mg  $\text{mL}^{-1}$  carrageenan in  $\text{H}_2\text{O}$  was prepared at 80 °C. This solution was sonicated three times for 30 min in melting ice (Heat Systems XL 2020 sonicator, 12 mm tip, power 475 W, frequency 20 kHz), the solution was centrifuged at elevated temperature to remove insoluble material. The sonicated materials were dialysed against phosphate buffer (20 mM  $\text{Na}_2\text{HPO}_4$ ;  $3 \times 2$  L), water ( $1 \times 2$  L) and lyophilised. Dialysis was performed to remove low-molecular-weight impurities that could disturb the NMR spectra. The material was dissolved at a concentration of 70–100 mg  $\text{mL}^{-1}$  in  $\text{D}_2\text{O}$  containing 20 mM  $\text{Na}_2\text{HPO}_4$  and 30 mM TSP. Chemical shifts ( $\delta$ ) are referred to a DSS standard ( $\delta_{\text{TSP}} = -0.170$  ppm relative to DSS for  $^{13}\text{C}$ ), and assignments of the NMR spectra were based on the literature data.<sup>25,27</sup>

### 2.4. Size-exclusion chromatography–multiangle laser light scattering (SEC–MALLS) analysis

Size-exclusion chromatography was performed at a constant flow rate of 1  $\text{mL min}^{-1}$  using TSK-gel 6000PW and TSK-gel 3000PW columns (Phenomenex) in series with a TSK guard column (Phenomenex). Detection was done simultaneously with a RI (refractive index) detector (ERC-7510 RI; Erma Optical Works Ltd.), an optical rotation detector (OR-1590 chiral detector; Jasco), and a multi-angle laser light scattering detector (Dawn DSP-F; Wyatt Technology Corp.). Data analysis was performed using ASTRA for Windows software (Wyatt Technology Corp.). The columns were thermostatted in a column oven (Waters chromatography). A programmable HPLC pump (LC-10AT; Shimadzu) with an in-line degassing unit (X-Act; Jour Research) was

**Table 1.** Source and composition of the collected crude carrageenan samples

ID <sup>a</sup>	Species <sup>b</sup>	Molecular composition based on <sup>1</sup> H NMR							Cation composition based on ICP–AES (mol-%) <sup>c</sup>				Supplier <sup>f</sup>	
		Composition of carrageenans (mol-%) <sup>c</sup>					Other (%) <sup>d</sup>		Na	K	Ca	Mg	Name	Code
		κ	ι	μ	ν	λ	Pyr.	n.i.						
K1	<i>Agardhiella</i> sp.	1	97				2	11	13	35	46	7	CP	BRR 23/1-03
K20	<i>Ahnfeltiopsis devoniensis</i> G	20	80						86	11	3	0	UC	174b
K17	<i>Ahnfeltiopsis devoniensis</i> G	17	81		2				92	6	3	0	UC	194
K29	<i>Ahnfeltiopsis devoniensis</i> G	29	71						90	6	4	0	UC	202
K35	<i>Ahnfeltiopsis devoniensis</i> G	35	65						83	14	2	0	UC	216a
K22	<i>Ahnfeltiopsis devoniensis</i> G	22	78						83	15	2	1	UC	216b
	<i>Caliblepharis jubata</i> NF	2	89		9			25	89	9	1	1	UC	101
K8	<i>Catenella impudica</i>	8	89	1			2		25	9	59	7	CP	S-4990-1
	<i>Chondracanthus teedei</i> FG	58	42					5	83	11	2	5	UC	113
K50	<i>Chondracanthus teedei</i> NF	50	50						82	2	8	7	UC	212a
K74	<i>Chondrus crispus</i>	75	25						5	85	8	2	CP	CNS XP 31-48
	<i>Chondrus crispus</i>	70	28	2				2	52	44	2	3	CP	CNS kappa/iota
	<i>Chondrus crispus</i>	64	36					6	43	52	5	n.d.	SKW	H1222B
K4	<i>Eucheuma denticulatum</i>	4	96					1	32	33	35	n.d.	CP	C-181
K3	<i>Eucheuma denticulatum</i>	4	96				4	12	43	54	4	n.d.	SKW	H1213
K83	<i>Eucheuma platycladum</i>	79	17	3	1				25	47	27	1	CP	S-4683
K62	<i>Gigartina skottsbergii</i>	59	41					1	15	60	15	10	CP	GSK kappa/iota
	<i>Grateloupia indica</i>	39	53				8	5	25	41	30	5	CP	S-5054-1
	<i>Gymnogongrus crenulatus</i> TB	64	31				5	11	88	10	2	1	CU	234b
K98	<i>Hypnea musciformis</i>	98	2					1	2	95	2	1	CP	1015-9A
K93	<i>Kappaphycus alvarezii</i>	93	7						6	93	1	n.d.	CP	U-004
K90	<i>Kappaphycus alvarezii</i>	90	10					1	35	64	1	n.d.	SKW	H4576
K55	<i>Mazaele laminarioides</i>	55	43	2					25	55	9	10	CP	GNK kappa/iota
	<i>Mazaele laminarioides</i> + <i>Sarcothalia crispata</i>	45	47				8	6	57	40	3	n.d.	SKW	H1194
	<i>Sarconema scinaoides</i>	4	68			2	26	14	4	11	79	6	CP	S-4981-1
K57	<i>Sarcothalia crispata</i>	57	42	1					53	39	1	7	CP	GBL kappa/iota

<sup>a</sup> ID used throughout this paper.

<sup>b</sup> FG = female gametophytes; G = gametophytes; NF = nonfructified thalli; TB = tetrasporoblastic thalli.

<sup>c</sup> Molar fraction of carrageenan repeating units.

<sup>d</sup> Integrated area relative to the total integrated area; n.i. = not identified.

<sup>e</sup> n.d. = not determined.

<sup>f</sup> CP = CP Kelco; UC = University of Coimbra; SKW = Degussa texturant systems.

used. An autosampler (Dilutor 401; Gilson) coupled to a waterbath (F3; Haake) was used for injection of the samples. Analysis of the carrageenans in the coil conformation was performed with a LiNO<sub>3</sub> solution (0.1 M) as eluent and a system temperature of 45 °C. Samples were prepared by adding MilliQ water (5 mL) to carrageenan (10 mg). After storage overnight at 4 °C, the samples were heated to 80 °C for 30 min. Before analysis the samples were diluted with a conc LiNO<sub>3</sub> solution to the concentration of the eluent.

### 2.5. Inductively coupled plasma–atomic emission spectrometry (ICP–AES) analysis

The cation composition of the crude and purified samples was determined by inductively coupled plasma–atomic emission spectrometry (ICP–AES analysis). Carrageenan (25 mg) was incinerated and subsequently

dissolved in sulfuric acid (1 mL; 65% wt/wt). After dilution with double-distilled water (9 mL), the samples were analysed using a Vista CCD simultaneous axial ICP–AES from Varian. Calibration was done with a multi-element solution containing Ca, K, Mg and Na.

### 2.6. Rheological measurements

Small-deformation measurements of storage modulus ( $G'$ ), loss modulus ( $G''$ ) and complex dynamic viscosity ( $\eta^* = (G'^2 + G''^2)^{1/2}/\omega$ , where  $\omega$  is frequency in rad/s) were performed using a Rheometrics Dynamic Stress Rheometer (SR 200, Rheometric Scientific Ltd., UK) with concentric cylinder geometry. The inner diameter was 29.5 mm, and the outer diameter was 32 mm. The inner cylinder had a length of 44.25 mm. Temperature was controlled by a Julabo circulating water bath and measured with a thermocouple attached to the stationary



element. Low concentrations of KCl and CaCl<sub>2</sub> were selected to combine reasonable  $G'$ -values with a low tendency for syneresis, thereby avoiding 'slip' between cup and cylinder. Carrageenan solutions (10 mg mL<sup>-1</sup>) in a mixed K<sup>+</sup>/Ca<sup>2+</sup>-solution (0.1% wt/wt KCl + 0.1% wt/wt CaCl<sub>2</sub>·2H<sub>2</sub>O, corresponding to 13.4 mM K<sup>+</sup> and 6.8 mM Ca<sup>2+</sup>) for small deformation oscillatory measurements were prepared from dried material, stored overnight at 4 °C and then heated to 95 °C for 10 min. Samples were loaded onto the rheometer in the solution state at 85 °C, and their periphery was coated with light silicone oil to minimise evaporation. They were then cooled to 8 °C, held for 150 min and re-heated to 85 °C. The heating and cooling scans were made at 1 °C min<sup>-1</sup>, with measurements of  $G'$  and  $G''$  at 1 Hz (6.28 rad/s). Stresses ( $\tau$ ) between 1 and 100 Pa, depending on the sample, were applied so that the resulting strain did not exceed the linear viscoelastic region.

### 2.7. Optical rotation measurements

The coil-to-helix transitions (cooling and heating curves) were monitored by optical rotation at 365 nm on a Jasco P1030 polarimeter in a jacketed cell with a 10-cm path length. The sample chamber was flushed with nitrogen to avoid condensation on the cell window at low temperatures. The temperature was controlled with a circulating refrigerated water bath (RTE 111, Neslab Inc.). Temperature and optical rotation were measured at 10-s intervals. Specific optical rotation values are given in degrees mM<sup>-1</sup> m<sup>-1</sup> (millimoles of repeating unit). Samples were prepared by dissolving (at 95 °C) carrageenan (2 mg mL<sup>-1</sup>) in a NaCl solution (0.2 M). The sample cell was equilibrated at 80 °C, filled with the hot carrageenan solution and subsequently cooled to 10 °C at a cooling rate of 0.5 °C min<sup>-1</sup>. The solution was held at 10 °C for 30 min and heated to 80 °C at a heating rate of 0.5 °C min<sup>-1</sup>.

For comparison with the rheological data, carrageenan (2 mg mL<sup>-1</sup>) was dissolved (at 95 °C for 30 min) in a mixed K<sup>+</sup>/Ca<sup>2+</sup> solution (0.1% wt/wt KCl + 0.1% wt/wt CaCl<sub>2</sub>·2H<sub>2</sub>O, corresponding to 13.4 mM KCl and 6.8 mM CaCl<sub>2</sub>). The sample cell was equilibrated at 85 °C, filled with the hot carrageenan solution and subsequently cooled to 5 °C at a cooling rate of 0.5 °C min<sup>-1</sup>. The solution was held at 5 °C for 70 min and heated to 85 °C at a heating rate of 1.0 °C min<sup>-1</sup>.

### 2.8. HSDSC measurements

Stock solutions of carrageenans were prepared by an incremental addition of the sample to water under continuous stirring and then left overnight to stand at room temperature. The carrageenan concentration in the stock solution was about 8 mg mL<sup>-1</sup>. This concentration

was determined by the dry residue method at 105 °C. Samples for calorimetric measurements with concentration of 4 mg mL<sup>-1</sup> were prepared by slowly adding 0.4 M NaCl to the stock solution. The solutions were stirred vigorously for 30–60 min, then placed into a hermetically closed vial and heated at 95 °C for 30 min immediately before the calorimetric experiment.

Reference mixtures of  $\iota$ - and  $\kappa$ -carrageenans of different compositions were prepared by mixing the stock solutions of samples K1 (99 mol-%  $\iota$ ) and K98 (98 mol-%  $\kappa$ ) with the subsequent dilution by 0.4 M NaCl to obtain a final carrageenan concentration of 4 mg mL<sup>-1</sup> in 0.2 M NaCl.

Calorimetric measurements were carried out with differential adiabatic scanning microcalorimeters, DASM-4 and DASM-4A (NPO 'Biopribor', Pushchino, Russia), in the temperature range of 10–80 °C under an excess pressure of 2 bar. The heating rate was 1.0 °C min<sup>-1</sup>. In each experiment, the measuring cell of the instrument was filled with the sample at a temperature of about 30 °C. Scans were done in triplicate. In most cases, the thermograms of the second and third scans coincided completely. As a rule, the results of the second scan were used for data processing.

The software package 'NAIRTA' (Institute of Biochemical Physics, Moscow) was used for data processing and calculation of the excess heat capacity functions of order-disorder transitions. The transition base line was approximated by a cubic polynomial. The transition temperature,  $T_i$  was determined as the peak temperature of excess heat capacity function. The transition enthalpy,  $\Delta_i h$ , was calculated by integration of the excess heat capacity function.

## 3. Results

### 3.1. Structural analysis and sample treatment

In order to study the effect of the  $\kappa/\iota$ -ratio on the properties of  $\kappa/\iota$ -hybrid carrageenans we collected a series of carrageenans extracted from a wide variety of red algae species (Table 1). These samples include commercial  $\kappa$ -carrageenan from *K. alvarezii*, commercial  $\iota$ -carrageenan from *E. denticulatum*,  $\kappa/\iota$ -hybrids from commercial sources, for example, *C. crispus* and *G. skottsbergii*, as well as homopolymeric  $\kappa$ - and  $\iota$ -carrageenan samples from, respectively, *H. musciformis* and *Agardhiella* sp. Moreover,  $\kappa/\iota$ -hybrids obtained from noncommercial sources completed this series to span the entire range from homopolymeric  $\kappa$ -carrageenan to homopolymeric  $\iota$ -carrageenan. All samples were analysed by <sup>1</sup>H NMR spectroscopy to determine the molecular ratio of different carrageenan repeating units.<sup>25,27</sup> The chemical shifts of the anomeric protons of the  $\alpha$ -linked units found for  $\kappa$ - and  $\iota$ -carrageenan were, respectively, 5.09 and

5.29 ppm, which is in agreement with literature data.<sup>27</sup> From Table 1 it is clear that the different algae species produce  $\kappa/\iota$ -hybrids with different  $\kappa/\iota$ -ratios. The  $\kappa/\iota$ -ratios observed for the  $\kappa/\iota$ -hybrids extracted from *C. crispus* (74 mol-%  $\kappa$ -units) and *G. skottsbergii* (62 mol-%  $\kappa$ -units) correspond with those reported.<sup>11</sup> This confirmed the general observation that red algae species produce a specific  $\kappa/\iota$ -hybrid, whose  $\kappa/\iota$ -ratio is independent of the seasonal variations, such as times and place of harvesting.

Although the crude samples were obtained by alkaline extraction, several samples contained small amounts of the precursor units  $\mu$ -carrageenan (5.24 ppm) and  $\nu$ -carrageenan (5.50 ppm). Samples containing these precursor units were subjected to an additional alkaline treatment to convert the  $\mu$ - and  $\nu$ -units into, respectively,  $\kappa$ - and  $\iota$ -units. Floridean starch (5.35 ppm), a branched (1 $\rightarrow$ 4,1 $\rightarrow$ 6)- $\alpha$ -D-glucan structurally related to plant amylopectins, was detected in many of the samples. Floridean starch is a water-soluble storage polysaccharide of red algae, which can accompany carrageenans in the extraction and precipitation steps.  $\alpha$ -Amylase was used to hydrolyse this contaminant, and a dialysis step was applied to remove the hydrolysis products. Pyruvic acid is a common component of many complex carrageenans. It forms a cyclic acetal at positions 4 and 6 of the 3-linked galactose residues.<sup>18,25,28</sup> The resonance of the anomeric proton of this substituted residue (5.49 ppm) coincides with that of  $\nu$ -carrageenan (5.50 ppm). In addition, the methyl protons give a characteristic resonance at 1.44 ppm (Fig. 2, trace 1). The

presence of the pyruvate acetal has been confirmed in the <sup>13</sup>C NMR spectrum of the carrageenan sample extracted from *Sarconema scinaoides*. Characteristic signals were observed at 27.6 ppm (methyl carbon) and 103.6 ppm (acetal carbon).<sup>27</sup> Pyruvate acetal substituents were detected in several of the samples, especially in those having a high content of  $\iota$ -carrageenan repeating units. As far as we know, no simple method is available to selectively remove the pyruvate acetals from the carrageenan chain. Therefore, samples containing significant amounts of pyruvate acetal groups were excluded from further analyses. In a final step, the samples were dialysed against NaCl solution to obtain the carrageenan samples in the sodium form. Due to the rather small quantities of carrageenans extracted from seaweeds collected at the Portuguese coast, these samples were used without further purification.

Subsequently, the purified samples (i.e., after consecutive  $\alpha$ -amylase treatment, alkaline treatment and dialysis) were analysed by <sup>1</sup>H NMR spectroscopy, size-exclusion chromatography (SEC-MALLS) and atomic emission spectroscopy (ICP-AES). Purified samples selected for further analysis are homogeneous  $\kappa/\iota$ -hybrid carrageenans containing less than 2% (mol) disturbing or precursor units, substituents or floridean starch, as determined by <sup>1</sup>H NMR spectroscopy (Fig. 2). The selected purified samples are summarised in Table 2 and plotted in a so-called ‘Stancioff diagram’ in Figure 3. The sample ID, which corresponds to the fraction of  $\kappa$ -repeating units, is used throughout this paper to distinguish the different samples. The results of the

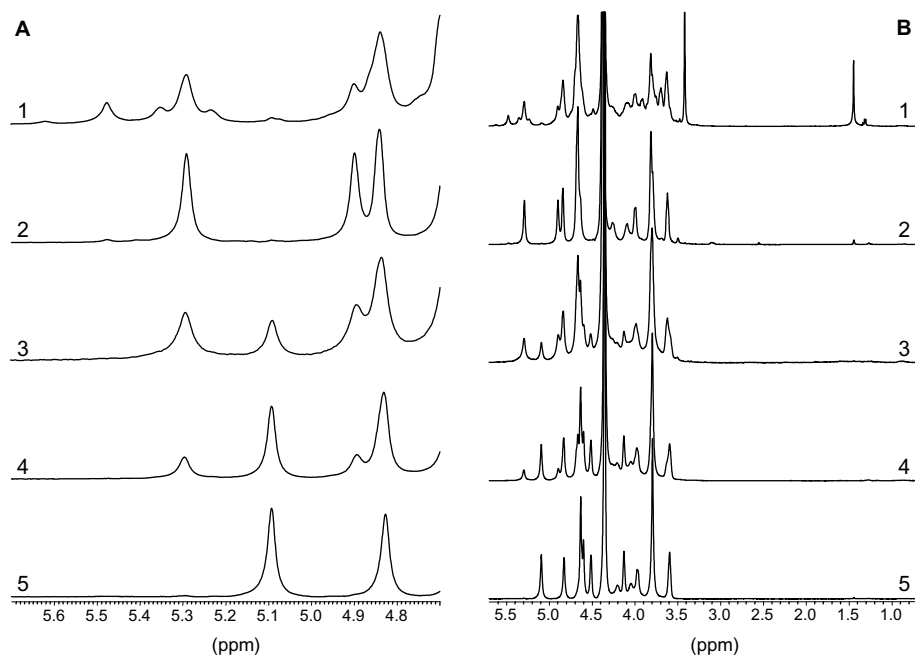


**Figure 2.** Anomeric proton region (A) and entire <sup>1</sup>H NMR spectra (B) of the crude carrageenan sample extracted from *Sarconema scinaoides* (1) and purified  $\kappa/\iota$ -hybrids of different compositions: K1 (2); K35 (3); K74 (4) and K98 (5).

**Table 2.** Composition of purified samples

Sample ID <sup>a</sup>	Species <sup>b</sup>	$\kappa$ content (mol-%) <sup>c</sup>	$M_w$ (kDa) <sup>d</sup>	Na content (mol-%) <sup>e</sup>
K1	<i>Agardhiella</i> sp.	1	175	98
K3	<i>Eucheuma denticulatum</i>	3	388	98
K4	<i>Eucheuma denticulatum</i>	4	256	99
K8	<i>Catenella impudica</i>	8	168	98
K17	<i>Ahnfeltiopsis devoniensis</i> G	17	n.d.	92
K20	<i>Ahnfeltiopsis devoniensis</i> G	20	656	86
K22	<i>Ahnfeltiopsis devoniensis</i> G	22	1020	83
K29	<i>Ahnfeltiopsis devoniensis</i> G	29	n.d.	90
K35	<i>Ahnfeltiopsis devoniensis</i> G	35	n.d.	83
K50	<i>Chondracanthus teedei</i> NF	50	1148	82
K55	<i>Mazaele laminarioides</i>	55	589	98
K57	<i>Sarcothalia crispata</i>	57	644	99
K62	<i>Gigartina skottsbergii</i>	62	411	97
K74	<i>Chondrus crispus</i>	74	599	98
K83	<i>Eucheuma platycladum</i>	83	370	98
K90	<i>Kappaphycus alvarezii</i>	90	404	98
K93	<i>Kappaphycus alvarezii</i>	93	444	98
K98	<i>Hypnea musciformis</i>	98	842	99

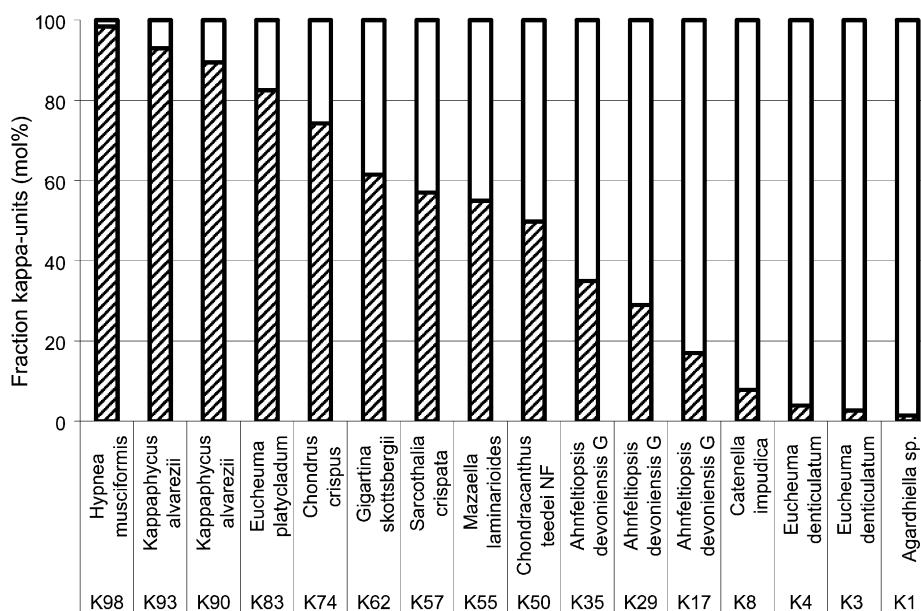
<sup>a</sup> ID used throughout this paper.

<sup>b</sup> G = gametophyte; NF = nonfructified thalli.

<sup>c</sup> Molar fraction determined by <sup>1</sup>H NMR spectroscopy.

<sup>d</sup> Determined by SEC–MALLS analysis; n.d. = not determined.

<sup>e</sup> Molar fraction from the cations present in the sample determined by ICP–AES analysis.

**Figure 3.**  $\kappa$ -content of purified  $\kappa/\lambda$ -hybrid carrageenans ('Stancioff diagram').

SEC–MALLS analysis showed a large variation in the molecular weight of the carrageenans, ranging from 168 to 1148 kDa. The molecular weight of the carrageenans depends on the sources as well as on the extraction procedure, as the Portuguese samples extracted under laboratory conditions represent the highest molecular weights. ICP analysis revealed that the sodium content of the samples after dialysis is above 95% (mol sodium ions per mol total cations).

### 3.2. Dynamic rheology

The dynamic moduli were determined in a mixed  $K^+$ / $Ca^{2+}$ -solution to lower the tendency for syneresis, thereby avoiding 'slip' between cup and cylinder. Although the  $\kappa$ -carrageenan formed a strong gel under these conditions,  $\lambda$ -carrageenan formed a weak gel. The storage modulus ( $G'$ ) and loss modulus ( $G''$ ) were measured at 1 Hz as a function of temperature for the series of

$\kappa/\iota$ -hybrid carrageenans (Fig. 4A). To assess linear response, the strain dependence of the storage modulus was measured at 8 °C. The observed  $G'$  was independent of the strain over the strain range 0.1–50% for several samples with different  $\kappa$ -contents (data not shown).

Under the selected salt conditions, homopolymeric  $\kappa$ -carrageenans form a firm gel with a  $G'$  of 15.5 kPa at 8 °C (after 2.5 h). Moreover, the storage modulus showed a continuous decrease with a decreasing fraction of  $\kappa$ -units in the  $\kappa/\iota$ -hybrid polymeric chain. Samples with a low fraction of  $\kappa$ -units formed weak gels. For example, sample K3 showed a  $G'$  of 0.04 kPa at 8 °C (Fig. 4). The gelation temperature, determined at the

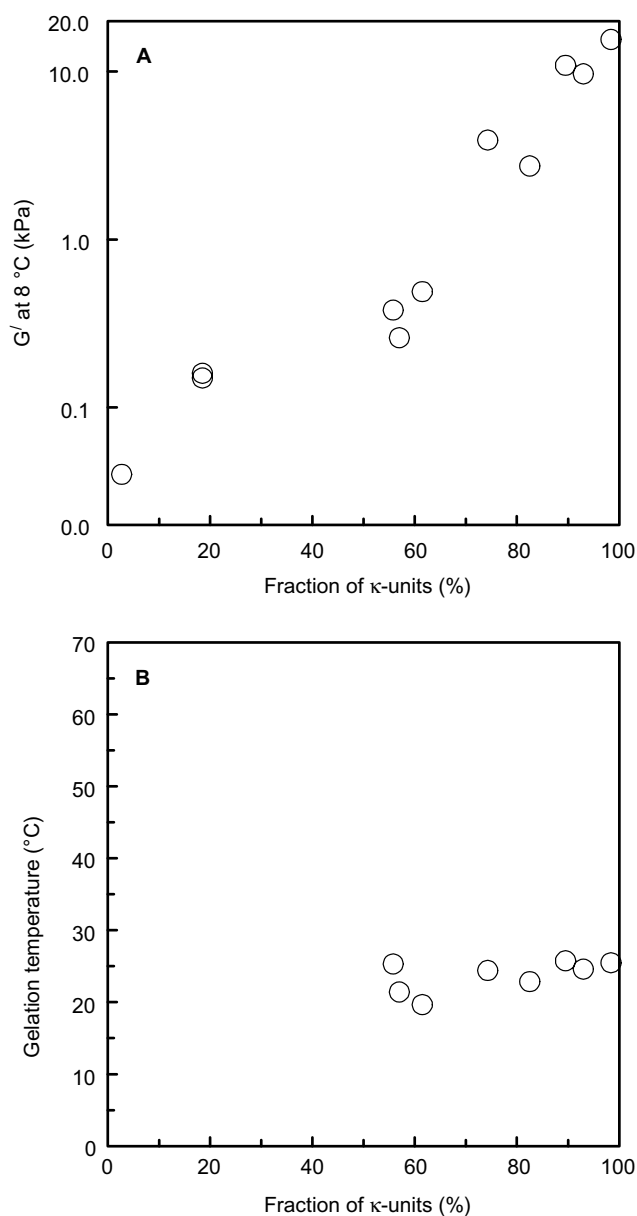


**Figure 4.** Storage modulus,  $G'$ , at 8 °C (A) and gelation temperature (B) as function of the fraction  $\kappa$ -units. Carrageenan concentration is 10 mg mL<sup>-1</sup> in 13.4 mM K<sup>+</sup> + 6.8 mM Ca<sup>2+</sup>.

crossover point of the storage and loss moduli ( $G' = G''$ , thus  $\tan(\delta) = 1$ ), as a function of the fraction  $\kappa$ -units is given in Figure 4B. Due to the low gel strength of the  $\iota$ -rich samples, Figure 4B shows only the gelation temperatures of the samples with a high  $\kappa$ -content. Little effect of the  $\kappa/\iota$ -ratio on the gelation temperature is observed. At high fraction of  $\kappa$ -units the gelation temperature is equal to that of homopolymeric  $\kappa$ -carrageenan ( $T_{\text{gel}} = 25$  °C). For homopolymeric  $\kappa$ -carrageenan the gelation temperature coincides with the onset temperature of the coil-to-helix transition observed by optical rotation at comparable ionic conditions (see Fig. 7A).

### 3.3. Optical rotation

Initially, optical rotation measurements were performed in the presence of 0.2 M NaCl as neither  $\kappa$ -carrageenan nor  $\iota$ -carrageenan shows specific affinity for sodium ions (see, for example, Piculell<sup>29</sup> and references cited therein). Moreover, under these ionic conditions the coil-to-helix transition of these carrageenans occur at different temperatures.<sup>1</sup> The optical rotation as a function of temperature (cooling curves) of homopolymeric  $\kappa$ - and  $\iota$ -carrageenan and some  $\kappa/\iota$ -hybrid samples is given in Figure 5. The coil-to-helix transition of homopolymeric  $\kappa$ - and  $\iota$ -carrageenan occurs at distinct temperatures. The onset temperatures were 22 and 57 °C for  $\kappa$ - and  $\iota$ -carrageenan, respectively. Also the shape of the curve is characteristic for each type of carrageenan. The transition temperatures as well as the shape of the curves are in good agreement with the literature data.<sup>30,31</sup> At high temperature the biopolymer molecules adopt the random

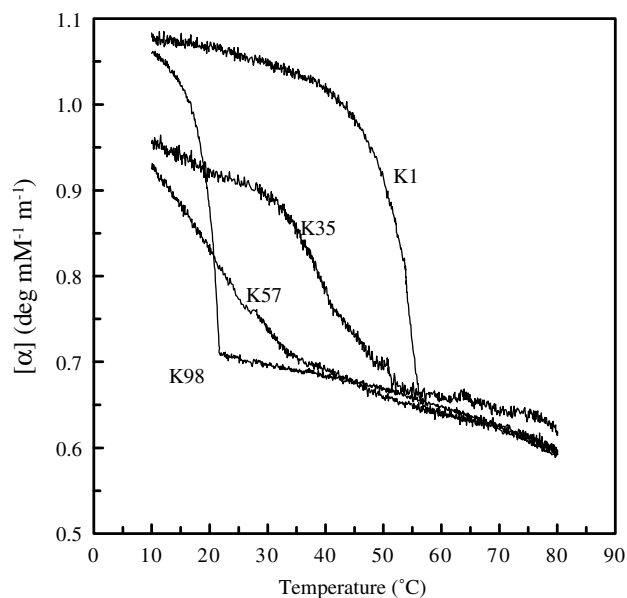


**Figure 5.** Optical rotation (cooling curves) versus temperature for  $\kappa/\iota$ -hybrid carrageenans with different  $\kappa/\iota$ -ratios as indicated in the graphs. Carrageenan concentration is 2 mg mL<sup>-1</sup> in 0.2 M NaCl.



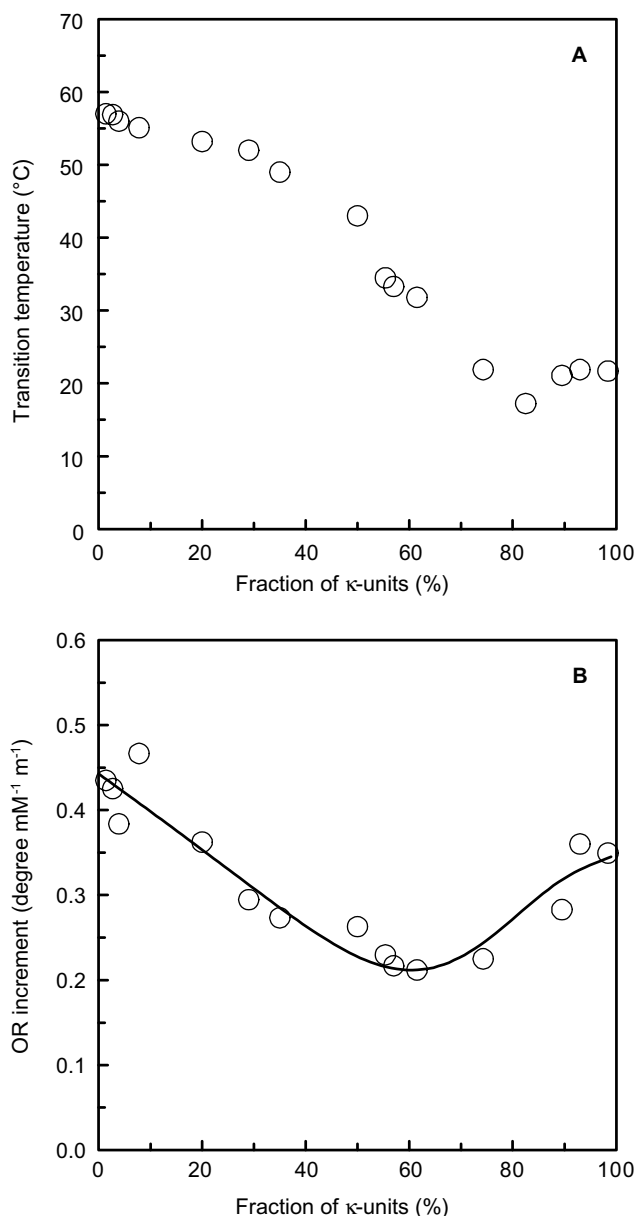


**Figure 6.** Disordered–ordered transition temperature (A) and the optical rotation increment (B), as a function of the fraction  $\kappa$ -units. Carrageenan concentration is  $2 \text{ mg mL}^{-1}$  in  $0.2 \text{ M NaCl}$ . The curve in panel B is calculated by the random block model (see text).

coil conformation (low optical rotation). The onset of the coil-to-helix transition of the homopolymeric carrageenans is observed as a sharp increase in optical rotation upon cooling. On further cooling, the optical rotation of the homopolymeric carrageenans reached a plateau value around  $10^\circ\text{C}$  (the limit of our measurement). This plateau value is assigned to that of the fully helical conformation.

From Figure 5 it is clear that the onset temperature of the coil-to-helix transition of the  $\kappa/\iota$ -hybrids depends on their composition. On the high  $\iota$ -content side of the series (samples K1–K50), an increasing amount of  $\kappa$ -units

is correlated with a decrease in transition temperature and a broadening of the transition. This is in agreement with the analysis of the coil-to-double helix transition of  $\iota$ -carrageenan based on the zipper model.<sup>32</sup> Interruption of the regularity of the chain induced by disturbing units leads to a decrease in the length of  $\iota$ -sequences. This decrease in the chain length leads to a lowering of the transition temperature.<sup>26</sup>

In Figure 6A the transition temperature is plotted against the fraction of  $\kappa$ -units present in the  $\kappa/\iota$ -hybrid chain. The transition temperature showed a gradual decrease from the high coil-to-helix transition temperature

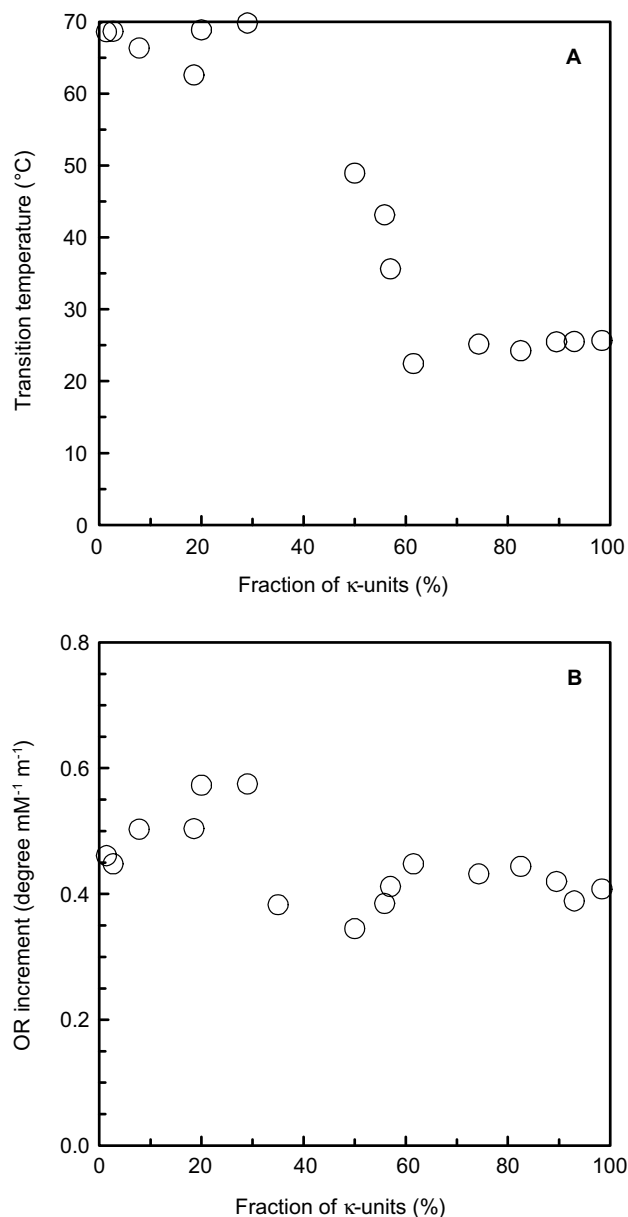


**Figure 7.** Disordered–ordered transition temperature (A) and optical rotation increment (B), as a function of the fraction  $\kappa$ -units for  $\kappa/\iota$ -hybrids in mixed salt solution. Carrageenan concentration is  $2 \text{ mg mL}^{-1}$  in  $13.4 \text{ mM KCl} + 6.8 \text{ mM CaCl}_2$ .

of homopolymeric  $\iota$ -carrageenan to the low coil-to-helix transition temperature of homopolymeric  $\kappa$ -carrageenan. The optical rotation increment is defined as the difference in specific optical rotation of the coil state (at high temperature) and the specific optical rotation of the helical state (at low temperature). The optical rotation increment as a function of the  $\kappa$ -content is given in Figure 6B. This optical rotation increment goes through a minimum at a  $\kappa$ -content of around 60 mol-%.

Additionally, optical rotation versus temperature curves were recorded in the mixed  $K^+/Ca^{2+}$ -solution used for the dynamic rheology measurements. Generally, the optical rotation versus temperature curves obtained in the mixed  $K^+/Ca^{2+}$  solution had a comparable shape to those obtained in  $Na^+$  solution. In contrast to the results obtained with sodium, the coil-to-helix transition temperature showed a discontinuous relation with the fraction of  $\kappa$ -units (Fig. 7A). At high fractions of  $\kappa$ -units the transition temperature is equal to that of homopolymeric  $\kappa$ -carrageenan (25 °C), whereas at low fractions of  $\kappa$ -units the transition temperature is equal to that of homopolymeric  $\iota$ -carrageenan (68 °C). At intermediate  $\kappa/\iota$ -ratios the transition temperature changed from that of homopolymeric  $\iota$ -carrageenan to homopolymeric  $\kappa$ -carrageenan while going from 40 to 60 mol-%  $\kappa$ -units. Moreover, the effect of the  $\kappa/\iota$ -ratio of the  $\kappa/\iota$ -hybrid carrageenans on optical rotation increment, measured in the mixed  $K^+/Ca^{2+}$  solution (Fig. 7B)

is less pronounced compared to the results obtained with  $Na^+$  solution. Although, a shallow minimum can be detected around 50%  $\kappa$ -units.

### 3.4. HSDSC measurements

High-sensitivity differential scanning calorimetry was used to study the helix-to-coil transition in the  $\kappa/\iota$ -hybrid carrageenan samples with different content of  $\kappa$ -units. As a preliminary, we studied simple mixtures of  $\iota$ - and  $\kappa$ -carrageenans of different compositions (Fig. 8A), in a NaCl solution (0.2 M). It is clear that the thermograms of the individual components, that is, homopolymeric  $\iota$ - and  $\kappa$ -carrageenans, are monomodal. Alternatively, thermograms of the mixtures are bimodal. The positions of their constituent peaks coincide with that of the peaks of the individual components. It is also seen that changes in the mixture composition result in regular changes in areas of the constituent peaks.

The thermograms of the  $\kappa/\iota$ -hybrids are also bimodal in the NaCl solution (Fig. 8B) as well as in the mixed  $K^+/Ca^{2+}$  solution (Fig. 8C). However, for most compositions the constituent peaks of thermograms were considerably overlapping. This hampered the precise determination of their thermodynamic parameters, for example, peak temperature and transition enthalpy. Therefore, the thermodynamic analysis was restricted to estimates of the transition temperatures for the

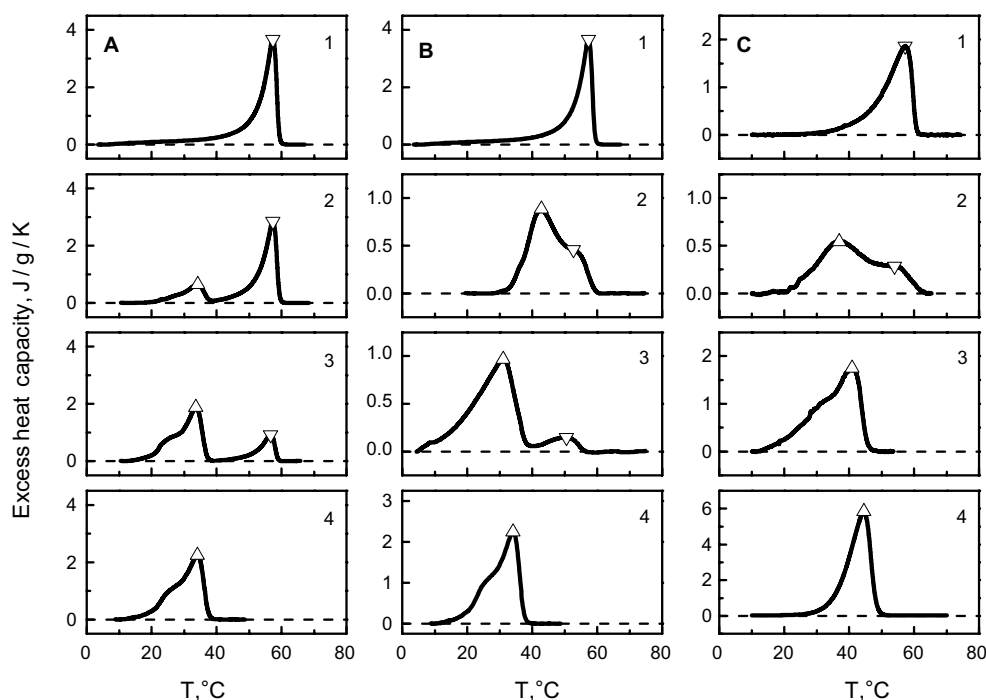
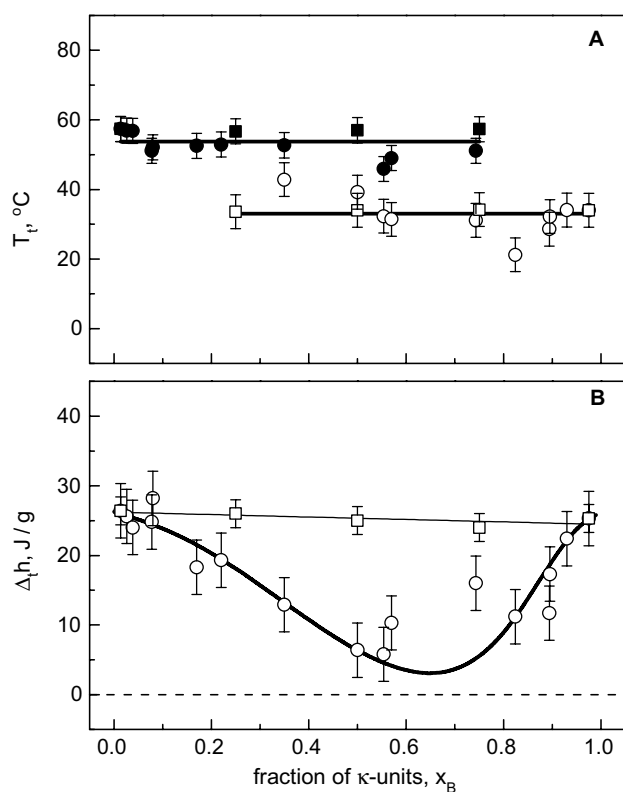


**Figure 8.** Excess heat capacity functions of order–disorder transitions in mixtures of  $\iota$ - and  $\kappa$ -carrageenans (A) and  $\iota/\kappa$ -hybrids carrageenan (B, C) of different compositions.  $\kappa$ -Carrageenan fraction is of 0.0 (1), 0.25 (2), 0.75 (3), 1.0 (4) for (A) and 0.0 (1), 0.35 (2), 0.74 (3), 0.98 (4) for (B) and (C);  $\nabla$ —transition temperature of  $\iota$ -carrageenan blocks,  $T_{i,A}$ ;  $\triangle$ —transition temperature of  $\kappa$ -carrageenan blocks,  $T_{i,B}$ . Experimental conditions: carrageenan concentration 4 mg mL<sup>-1</sup>; heating rate 1 °C min<sup>-1</sup>; 0.2 M NaCl (A and B); 13.4 mM KCl + 6.8 mM CaCl<sub>2</sub> (C).

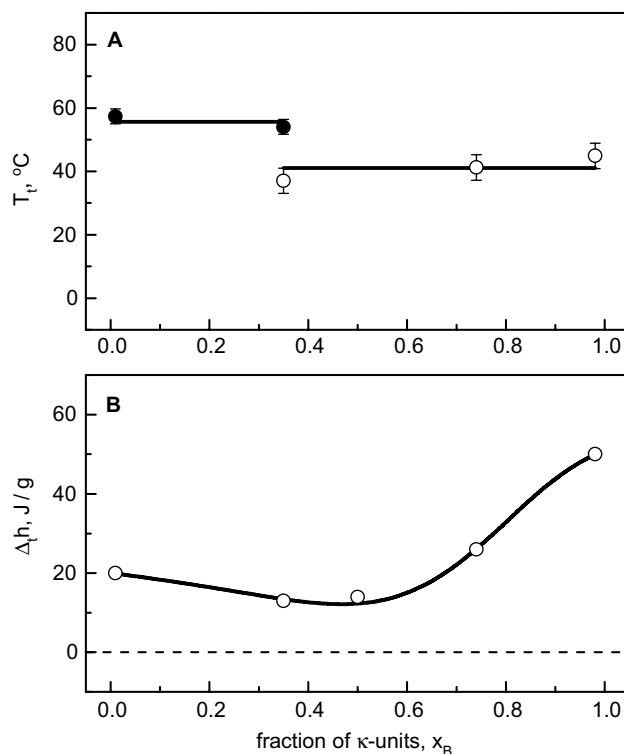
constituent peaks (marked by triangles in Fig. 8) and to the total transition enthalpy. The positions of the constituent peaks and evolution of the profile of the thermograms with changing  $\kappa/\iota$ -hybrid composition suggest that the low-temperature ( $\Delta$ ) and high-temperature ( $\nabla$ ) peaks can be ascribed to the transitions in the  $\kappa$ -blocks and  $\iota$ -blocks, respectively.

Figure 9 shows the dependences of transition temperatures (Panel A) and the total transition enthalpy (Panel B) on  $\kappa$ -carrageenan content for the simple mixtures. Evidently, the transition temperatures of the constituent peaks of the thermograms coincide with the transition temperatures of the individual components. The total transition enthalpy is a linear function of the mixture composition. These results illustrate a general behaviour of simple mixtures—the absence of mutual influence of the components. Figures 9 and 10 show that the  $\kappa/\iota$ -hybrids behave quite differently.

The transition temperatures of  $\iota$ - and  $\kappa$ -blocks do not undergo variations upon changing the  $\kappa/\iota$ -hybrid composition (Fig. 9A). Their average values are close to



**Figure 9.** Transition temperatures (A) and total transition enthalpy (B) of simple  $\iota/\kappa$ -carrageenan mixtures and  $\iota/\kappa$ -carrageenan hybrid samples versus molar fraction of  $\kappa$ -carrageenan repeating units in 0.2 M NaCl. A:  $\blacksquare$ — $\iota$ -blocks in the simple mixtures;  $\square$ — $\kappa$ -blocks in the simple mixtures;  $\bullet$ — $\iota$ -blocks in the hybrids;  $\circ$ — $\kappa$ -blocks in the hybrids; lines represent the global average transition temperatures for  $\iota$ - and  $\kappa$ -blocks; B:  $\square$ —simple mixtures;  $\circ$ —hybrids; the thin line is the additive approximation for the simple mixtures; the thick line is calculated by the random block model (see text).



**Figure 10.** Transition temperatures (A) and total transition enthalpy (B) of  $\iota/\kappa$ -carrageenan hybrid samples versus molar fraction of  $\kappa$ -carrageenan repeating units in 0.1% KCl + 0.1%  $\text{CaCl}_2 \cdot 2\text{H}_2\text{O}$ . A:  $\bullet$ — $\iota$ -blocks;  $\circ$ — $\kappa$ -blocks; lines represent the global average transition temperatures for  $\iota$ - and  $\kappa$ -blocks; B: the curve is calculated by the random block model (see text).

the transition temperatures of individual  $\iota$ - and  $\kappa$ -carrageenans and that of the mixtures of homopolymeric  $\kappa$ - and homopolymeric  $\iota$ -carrageenan (Table 3). In this respect the  $\kappa/\iota$ -hybrids behave similarly to the simple mixtures. A particular property of the  $\kappa/\iota$ -hybrids is the dependency of the total transition enthalpy on  $\kappa/\iota$ -hybrid composition. This dependency goes through a minimum at a molar fraction of  $\kappa$ -units of 0.6. In contrast, the total transition enthalpy of the mixtures of homopolymeric  $\kappa$ - and homopolymeric  $\iota$ -carrageenan is a linear function of the mixture composition (given by curve 3 in Fig. 9B).

Similar features of the  $\kappa/\iota$ -hybrids were observed in the presence of potassium and calcium cations that are promoters of gelation of  $\kappa$ - and  $\iota$ -carrageenans, respectively (Fig. 10). Similar to the results obtained in the presence of sodium, the transition temperatures of  $\iota$ - and  $\kappa$ -blocks are equal to those of homopolymeric  $\kappa$ -carrageenan and homopolymeric  $\iota$ -carrageenan. Moreover, the dependence of the total transition enthalpy on  $\kappa/\iota$ -hybrid composition goes through a minimum (Fig. 10B), although, this minimum is less pronounced compared to the results obtained in NaCl solution. This is in agreement with the results obtained by optical rotation measurements.

**Table 3.** Summary of the thermodynamic and model parameters of the model of random length distribution for sequences in different carrageenans

Carrageenan <sup>a</sup>	Condition	Sequence	Thermodynamic parameters		Model parameters of random block distribution model		
			$T_t$ (°C)	$\Delta_t h$ (J/g)	$\Delta_t h$ (J/g)	Critical sequence length ( $n^*$ )	
						HSDSC <sup>b</sup>	OR <sup>c</sup>
Homopolymers	0.2 M NaCl	$\kappa$ -Sequence	$34.0 \pm 0.2$	$25 \pm 2$			
		$\iota$ -Sequence	$57.1 \pm 0.3$	$26 \pm 2$			
$\kappa/\iota$ -Hybrid	0.2 M NaCl	$\kappa$ -Sequence	$33 \pm 6$		$26 \pm 3$	$14 \pm 3$	$\sim 8$
		$\iota$ -Sequence	$53 \pm 4$		$26 \pm 2$	$5 \pm 1$	$\sim 2$
Homopolymers	13.4 mM KCl + 6.8 mM CaCl <sub>2</sub>	$\kappa$ -Sequence	$45 \pm 2$	$50 \pm 3.3$			
		$\iota$ -Sequence	$57 \pm 2$	$20 \pm 3.3$			
$\kappa/\iota$ -Hybrid	13.4 mM KCl + 6.8 mM CaCl <sub>2</sub>	$\kappa$ -Sequence	$41 \pm 4$		$52 \pm 2$	$8 \pm 2$	
		$\iota$ -Sequence	$56 \pm 2$		$20 \pm 2$	$2 \pm 1$	
$\nu/\iota$ -Hybrid	0.8 M NaCl	$\nu$ -Sequence <sup>d</sup>				n.a.	n.a.
		$\iota$ -Sequence				$30 \pm 2$	$23 \pm 2$

<sup>a</sup> Data for the homopolymeric and  $\kappa/\iota$ -hybrid carrageenans obtained within this study; data for the  $\nu/\iota$ -hybrid from Van de Velde et al.<sup>26</sup>

<sup>b</sup> Critical sequence lengths obtained for high-sensitivity differential scanning calorimetry, carrageenan concentration 4 mg mL<sup>-1</sup>.

<sup>c</sup> Critical sequence lengths obtained for optical rotation measurements, carrageenan concentration 2 mg mL<sup>-1</sup>.

<sup>d</sup> n.a.: not applicable as  $\nu$ -sequences do not form double helices.

### 3.5. Random length distribution model

To analyse the dependence of the total transition enthalpy of the  $\kappa/\iota$ -hybrids on their composition, we suggest that the  $\kappa/\iota$ -hybrids are random AB block copolymers. In that case, there are length distribution functions for AA and BB sequences,  $W_A(n)$  and  $W_B(n)$ , as a function of copolymer composition (see Computations section). Then we suggest that only sequences with a specific minimum length can participate in cooperative conformational transitions. The minimum number of repeating units necessary for a conformational transition is defined as the critical sequence length,  $n_A^*$  and  $n_B^*$  for, respectively,  $\iota$ - and  $\kappa$ -carrageenan sequences. Thus, the total transition enthalpy can be expressed as a function of the  $\kappa/\iota$ -hybrid composition and the critical length of the  $\kappa$ - and  $\iota$ -sequences.

The random length distribution model (Eqs. 1–5 in Computations section) could be satisfactorily fitted to the experimental dependences of the total transition enthalpy on  $\kappa/\iota$ -hybrid composition (bold lines in Figs. 9B and 10B). The model parameters for  $\iota$ - and  $\kappa$ -sequences (AA and BB sequences, respectively), obtained as a result of the fit, are summarised in Table 3. Note that the subscripts A and B refer to, respectively, the  $\iota$ - and  $\kappa$ -sequences in  $\kappa/\iota$ -hybrids, whereas the subscripts  $\iota$  and  $\kappa$  are used to identify the homopolymeric  $\iota$ - and  $\kappa$ -carrageenan. The intrinsic parameters of  $\iota$ - and  $\kappa$ -sequences, for example, the transition temperatures and specific transition enthalpies, agree well with the corresponding parameters of individual homopolymeric  $\iota$ - and  $\kappa$ -carrageenans. Moreover, the critical lengths of  $\kappa$ -sequences are considerably larger than those of  $\iota$ -sequences. The calculated critical length of  $\kappa$ -sequences in the presence of potassium ions is in accordance with

the results of the direct spectroscopic data of Rochas et al.<sup>33</sup> on  $\kappa$ -carrageenan oligomers,  $n^* \sim 8$ –9.

In addition to the total transition enthalpies of the  $\kappa/\iota$ -hybrids, the optical rotation increments (Figs. 6B and 7B) were fitted using the same formalism (Eq. 6 in Computations section). This relation describes well the experimental data for  $\kappa/\iota$ -hybrids in 0.2 M NaCl at  $n_A^* \sim 2$  and  $n_B^* \sim 8$  (curve in Fig. 6B). Note that again  $n_A^* < n_B^*$ , but the values are smaller than those obtained from the calorimetric data. The results of these fits are included in Table 3. Moreover, from Figures 5 and 6B it is clear that the onset temperature of the coil-to-helix transition of the  $\kappa/\iota$ -hybrids is dependent on their composition. On the high  $\iota$ -content side of the series (samples K1–K50), an increasing amount of  $\kappa$ -units showed a decrease in transition temperature and a broadening of the transition.

This random block formalism has been applied to consider the HSDSC and OR data of  $\nu/\iota$ -carrageenans, for example, copolymers of  $\iota$ - and  $\nu$ -repeating units.<sup>26</sup> It is of importance to mention that  $\nu$ -sequences do not form double helices. Only one peak corresponding to the transition of  $\iota$ -carrageenan was observed in the thermograms of  $\nu$ -carrageenans. The total transition enthalpy as well as the optical rotation increment of  $\iota$ -carrageenan drop quickly with increasing content of  $\nu$ -units (see Figs. 5 and 12 in Van de Velde et al.<sup>26</sup>). The peak of the total transition enthalpy disappeared at a content of  $\nu$ -units larger than 10 mol-%. Within experimental error the transition temperatures of  $\nu$ -carrageenans agreed with that of  $\iota$ -carrageenan. The total transition enthalpy went down quickly with increasing content of  $\nu$ -units. An attempt to approximate this dependence by the random block model was less convincing than that for the  $\kappa/\iota$ -hybrids (not shown).

Possibly, this was due to the fact that in the transient range of content of  $\nu$ -units (of about 10%) values of the transition enthalpy were too small to be detected by the instrument used. Nevertheless, we could determine a critical length of  $\nu$ -sequences in  $\nu$ -carrageenans with reasonable precision:  $n_A^* = 30 \pm 2$  (Table 3).

### 3.6. Hysteresis

Hysteresis is defined as the temperature difference between the transition temperature measured upon heating and cooling. Hysteresis is generally observed in the presence of aggregation-promoting ions, such as  $K^+$  in the case of  $\kappa$ -carrageenan. The hysteresis behaviour of  $\kappa/\iota$ -hybrid carrageenans has been measured by optical rotation measurements and HSDSC, as well as in the two different salt solutions. The hysteresis observed is plotted as a function of the fraction of  $\kappa$ -units in the  $\kappa/\iota$ -hybrid carrageenans for these two salt solutions (Fig. 11). This figure shows the dependency of the degree of hysteresis on the fraction  $\kappa$ -units. In 0.2 M NaCl a maximum hysteresis of 16 °C is observed for homopolymeric  $\kappa$ -carrageenan. The hysteresis showed a steep decrease by decreasing the fraction of  $\kappa$ -units in the molecular chain. No hysteresis is observed below a  $\kappa$ -content of 80 mol-%. In the mixed  $K^+/Ca^{2+}$  solution the maximum hysteresis is 28 °C. With increasing fraction of  $\iota$ -units the observed hysteresis decreased and below a  $\kappa$ -content of 50% the transition temperatures measured upon heating and cooling were equal. Although calcium ions induce helix formation of

$\iota$ -carrageenan, hysteresis in  $\iota$ -rich samples was not observed in the mixed  $K^+/Ca^{2+}$  solution.

## 4. Discussion

The hybrid nature of  $\kappa/\iota$ -hybrid carrageenans has been demonstrated by KCl-fractionation techniques for samples extracted from *C. crispus* and *M. laminarioides/S. crispata*.<sup>1</sup> Although this fractionation technique has not been applied to the series of  $\kappa/\iota$ -hybrids presented in this study, the difference in the  $\kappa/\iota$ -ratio dependence of the transition enthalpy between the hand-made mixtures and the  $\kappa/\iota$ -hybrids (Fig. 9B) indicates strongly that the studied samples are  $\kappa/\iota$ -hybrids. The total transition enthalpy of the hand-made mixtures is a linear function of the mixture composition. In contrast to the simple mixtures, the total transition enthalpy of the  $\kappa/\iota$ -hybrids is dependent on the  $\kappa/\iota$ -hybrid composition. The transition enthalpy goes through a minimum. Therefore, the  $\kappa/\iota$ -hybrid carrageenan samples used within the current study are regarded as mixed chain or heteropolymeric carrageenans comprising both  $\kappa$ - and  $\iota$ -repeating units on the same polymeric chain. This study aimed at understanding the composition dependence of the functional properties, for example, gel strength, as well as the coil-to-helix transition of  $\kappa/\iota$ -hybrid carrageenans.

To this end we collected a series of  $\kappa/\iota$ -hybrid carrageenans extracted from a wide variety of red algae species (Table 1). <sup>1</sup>H NMR spectroscopy was used to determine the molecular ratio of the different carrageenan repeating units and contaminants. After purification a unique series of  $\kappa/\iota$ -hybrid carrageenans was obtained ranging from homopolymeric  $\kappa$ -carrageenan to homopolymeric  $\iota$ -carrageenan (Fig. 3). The purified samples contained less than 2 mol-% disturbing or precursor units as determined by <sup>1</sup>H NMR spectroscopy (Fig. 2), and their sodium content was above 95 mol-%. The only complicating factor was the large variation in the weight-average molecular weight of the samples, which ranged from 168 to 1148 kDa, depending on the source and the extraction procedure.

As carrageenans represent one of the major texturising ingredients, their rheological properties are of key importance. Although gel break force or penetration tests of either water or milk gels are generally applied to study the functional properties of these  $\kappa/\iota$ -hybrids,<sup>8,10,12</sup> we preferred to use small deformation oscillatory rheology to measure the storage modulus ( $G'$ ) and loss modulus ( $G''$ ) of the  $\kappa/\iota$ -hybrids as a function of temperature. Moreover, small deformation rheology offers the advantage of relatively small sample volumes compared to gel break force measurements and penetration tests. The storage modulus of homopolymeric  $\kappa$ -carrageenan (15.5 kPa) thus obtained is in agreement

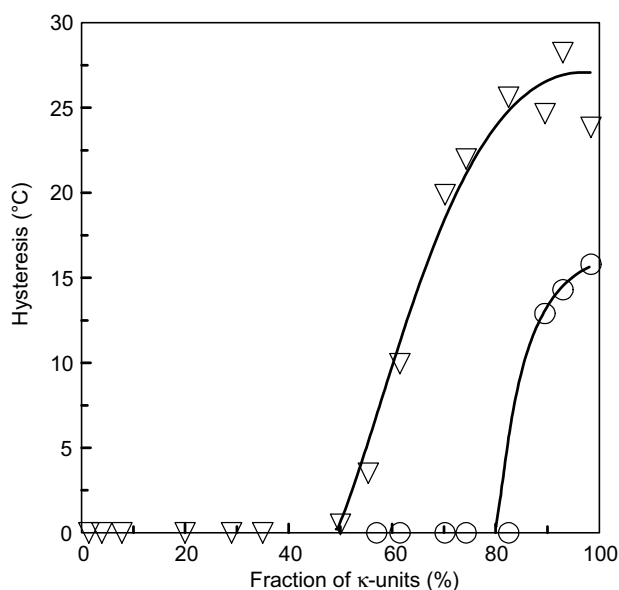


**Figure 11.** Hysteresis as measured by optical rotation versus molar fraction of  $\kappa$ -units. Experimental conditions: ○: 0.2 M Na<sup>+</sup>; △: 3.4 mM KCl + 6.8 mM CaCl<sub>2</sub>; carrageenan concentration 2 mg mL<sup>-1</sup>.



with the literature data measured under comparable conditions.<sup>34,35</sup> Under the ionic conditions used for the rheological measurements, the samples with a high  $\kappa$ -content form a macroscopic gel upon cooling, whereas the  $\iota$ -rich samples remain a viscous liquid at low temperatures. The storage modulus decreases with decreasing fraction of  $\kappa$ -units (Fig. 4A). In contrast, the gelation temperature is independent of composition of the  $\kappa/\iota$ -hybrid carrageenans (Fig. 4B). A further comparison of our results with the literature data is complicated as the temperature dependence of this data is not included in these publications. Moreover, the cation compositions of the samples is not taken into account and several extraction procedures, for example, NaOH and Ca(OH)<sub>2</sub>, have been applied.<sup>10</sup>

The issue of the ordered conformation of gelling carrageenans has been intensively studied during the last decades. The presence of an ordered conformation as a prerequisite for the gelation of carrageenans as proposed by D. A. Rees is nowadays generally accepted (see, for example, Piculell<sup>29</sup> and references cited therein). Thus, the first step in carrageenan gelation at moderate concentrations is an ion-induced, thermoreversible transition from a disordered (coil) state to an ordered (helical) state. In the second step a space-filling network is formed through aggregation of these helices upon increasing the carrageenan concentration or ionic strength or a decrease in temperature. However, the nature of the ordered conformation is still a matter of debate, either being a single or double helical state. The existence of the single helices as the ordered conformation of both  $\kappa$ - and  $\iota$ -carrageenan has been established at low polymer concentrations using light and X-ray scattering techniques (LALLS, WALLS and SAXS).<sup>36–38</sup> These single helices or single-helical regions aggregate into large aggregates of multiple helices to form a gel upon increasing salt or carrageenan concentration or decreasing temperature. On the other hand, X-ray fibre diffraction data showed a double-helical structure for both  $\kappa$ - and  $\iota$ -carrageenan in the solid state.<sup>39–41</sup> The double helix is also supported by a doubling of the observed molecular weight of carrageenans while going from the disordered to the ordered state.<sup>42</sup> In addition, the specific optical rotation of the ordered conformation of potassium  $\iota$ -carrageenan in solution coincides exactly with the calculated value for the double helix.<sup>43</sup> Moreover, the formation of the  $\iota$ -carrageenan double helix follows second-order reaction kinetics.<sup>44</sup> As for the single-helical model, the double helices aggregate to form junction zones that are responsible for the gel formation of carrageenans.

A comprehensive survey of the literature on the ongoing debate about the nature of the ordered state reveals that this debate is focussed on  $\kappa$ - and  $\iota$ -carrageenan. Most studies use commercial  $\kappa$ -carrageenan extracted from *K. alvarezii*<sup>37</sup> or commercial  $\iota$ -carrageenan ex-

tracted from *E. denticulatum*,<sup>38</sup> although these carrageenans contain generally 5–10% impurities of each other (see Table 1 in this paper and Table 1 in Van de Velde et al.<sup>1</sup>). The present study comprises these samples from commercial origin as well as homopolymeric  $\kappa$ - and  $\iota$ -carrageenan and a series of  $\kappa/\iota$ -hybrids. The coil-to-helix transition of this series has been studied from a thermodynamics point of view. The excess heat capacity curve of  $\iota$ -carrageenan (Fig. 7) clearly shows a second-order phase transition. The double helix-to-coil transition is a second-order phase transition and, therefore, the results of this study were analysed according to the concept of double helices being the ordered structure of both  $\iota$ - and  $\kappa$ -carrageenan.

The random length distribution model (Eqs. 1–5 in Computations section) was used to analyse the dependence of the total transition enthalpy and the optical rotation increments of the  $\kappa/\iota$ -hybrids on their composition. This analysis results in the critical sequence lengths necessary for a conformational transition,  $n_A^*$  and  $n_B^*$  for, respectively,  $\iota$ - and  $\kappa$ -carrageenan sequences (Table 3). This random block formalism was also applied to consider the HSDSC and OR data of  $\nu/\iota$ -carrageenans, for example, copolymers of  $\iota$ - and  $\nu$ -repeating units.<sup>26</sup> Based on the results of the analyses (Table 3), four observations can be made:

1. The value for the critical sequence length of  $\kappa$ -sequences is higher than that of the  $\iota$ -sequences.
2. The value for the critical lengths of the sequences in these  $\kappa/\iota$ -hybrids tend to decrease in the presence of calcium and potassium ions that are promoters of ordering and gelation in  $\iota$ - and  $\kappa$ -carrageenan, respectively.
3. The value for the critical length of the  $\iota$ -sequences in the  $\nu/\iota$ -hybrids is much higher than that in the  $\kappa/\iota$ -hybrids.
4. The value for the critical lengths calculated from the OR data are smaller than those calculated from the HSDSC data.

Firstly, the calculated value for the critical sequence length of  $\kappa$ - and  $\iota$ -sequences of  $\kappa/\iota$ -hybrids is discussed. The critical lengths of  $\kappa$ -sequences are larger than those of  $\iota$ -sequences. It is of interest to consider relationships between the values that were obtained for the critical lengths in more detail. The critical length of a helical sequence is supposed to be directly related with its nucleation constant,  $\sigma$ .<sup>45</sup> A small value for  $\sigma$  is related to a large critical length. Thus, comparing the critical lengths of  $\iota$ - and  $\kappa$ -sequences one could expect that the nucleation constant of the  $\iota$ -sequences should be larger than that of the  $\kappa$ -sequences. To verify this suggestion we performed calorimetric experiments with highly purified reference samples of homopolymeric  $\iota$ - and  $\kappa$ -carrageenan in 0.2 M NaCl. The integral transition curves

(not shown) were analysed in terms of a model of double helix-coil transition.<sup>44</sup> The estimated  $\sigma$ -values were for  $\iota$ -carrageenan  $\sigma = 1.0 \pm 0.2$  and for  $\kappa$ -carrageenan  $\sigma = 0.5 \pm 0.1$ . Hence, one can assert that under comparable conditions the length distribution of  $\iota$ -helices relative to that of  $\kappa$ -helices is shifted towards smaller lengths, because of smaller cooperativity of formation of  $\iota$ -helices.

Secondly, the value for the critical length of  $\iota$ - and  $\kappa$ -sequences in the  $\kappa/\iota$ -hybrids tend to decrease in the presence of the potassium and calcium cations. These cations promote the gelation of the carrageenans and thereby stabilise the helical conformation. A stabilised helical conformation reduces the number of units necessary to form a stable double helix. This explains the decreased value for the critical lengths of the  $\iota$ - and  $\kappa$ -sequences in the presence of the potassium and calcium cations. Our estimate of the value for the critical length of  $\kappa$ -sequences in the presence of potassium cations is compatible with the results of direct experiments of Rochas et al.<sup>33</sup>

Thirdly, in the case in  $\nu/\iota$ -hybrids, the value for the critical length of the  $\iota$ -sequences is much higher than that in  $\kappa/\iota$ -hybrids. In the case of the  $\nu/\iota$ -hybrids, not only the nucleation constant ( $\sigma_{\text{iota}}$ ) is of importance, but also the behaviour of  $\iota$ -units at the  $\iota/\nu$ -interfaces needs to be taken into account. Therefore, the conformation of the 4-linked galactose residues in the different hybrids is of importance. In the  $\kappa/\iota$ -hybrids the 4-linked galactose residue of both  $\kappa$ - and  $\iota$ -units, respectively, DA and DA2S, adopt the  ${}^1C_4$ -chair conformation. This conformation, that results from the 3,6-anhydro bridge, is crucial for the formation of the helical structure. On the other hand, the D2S,6S residues of the  $\nu$ -units in the  $\nu/\iota$ -hybrids, which lack the 3,6-anhydro bridge, adopt the  ${}^4C_1$ -chair conformation and disturb the helical conformation.<sup>46</sup> Since the  $\nu$ -units are not able to form an ordered helical structure, helix nucleation of  $\iota$ -units at the  $\iota/\nu$ -interface should be unlikely. To all appearances this should result in a much higher critical sequence length. This explains the large difference in the critical lengths of the  $\iota$ -sequences in the  $\kappa/\iota$ -hybrids and  $\nu/\iota$ -hybrids. Moreover, it explains the relative strong dependence of the physical properties of  $\nu/\iota$ -carrageenan on their composition<sup>26</sup> compared to those of the  $\kappa/\iota$ -hybrid carrageenans presented in this study.

Finally, high-sensitivity differential scanning calorimetry and optical rotation are able to estimate the critical lengths in different ways. HSDSC due to its dynamic origin can detect cooperative transitions with an appropriate excess heat capacity, which are typical for long sequences. OR measurements do not suffer from these limitations. Optical rotation detects every change in chirality including noncooperative ones. Thus HSDSC detects only the cooperative double helix-to-coil transitions, whereas optical rotation reflects also the noncoop-

erative transition typical for very short sequences. Consequently, the value for the critical length determined by HSDSC has to be higher than that determined by OR measurements.

## 5. Computations

To analyse the dependence of the total transition enthalpy of the  $\kappa/\iota$ -hybrids on their composition, we suggest that the  $\kappa/\iota$ -hybrids are random AB block copolymers. In that case, there are length distribution functions for AA and BB sequences,  $W_A(n)$  and  $W_B(n)$ , as a function of copolymer composition:<sup>47</sup>

$$W_A(n) = (1 - v_{AA})^2 n v_{AA}^{n-1} \quad (1a)$$

$$W_B(n) = (1 - v_{BB})^2 n v_{BB}^{n-1} \quad (1b)$$

where

$$v_{AA} = 1 - L_A^{-1} \quad (2a)$$

$$v_{BB} = 1 - L_B^{-1} \quad (2b)$$

$$L_A = \frac{2x_A}{x_{AB}} \quad (3a)$$

$$L_B = \frac{2x_B}{x_{AB}} \quad (3b)$$

$x_A$  and  $x_B$  are molar fractions of A and B repeating units, and  $x_{AB}$  is a fraction of AB junctions in primary structure of the copolymer. For a random block copolymer  $x_{AB} = 2x_A x_B$ .

Then we suggest that only enough long sequences can participate in the conformational transitions. In other words, we are interested in the length distribution functions truncated from the side of small lengths. We call a truncating limit expressed in the number of repeating units as a critical sequence length,  $n_A^*$  and  $n_B^*$  for AA and BB sequences.

Thus we can express the total specific transition enthalpy as a function of critical lengths of AA and BB sequences and copolymer composition:

$$\begin{aligned} & \Delta_t h(n_A^*, n_B^*, x_B) \\ &= \frac{\Delta_t h_A M_A \delta_A(n_A^*, x_B)(1 - x_B) + \Delta_t h_B M_B \delta_B(n_B^*, x_B)x_B}{M_A(1 - x_B) + M_B x_B} \end{aligned} \quad (4)$$

where  $\delta_A(n_A^*, x_B)$  and  $\delta_B(n_B^*, x_B)$  are fractions of A and B repeating units participating in the transitions;  $\Delta_t h_A$  and  $\Delta_t h_B$  are transition enthalpies of AA and BB

blocks per repeating unit;  $M_A$  and  $M_B$  are molecular weights of A and B repeating units. According to the definition,

$$\delta_A(n_A^*, x_B) = \frac{\sum_{n=n_A^*}^{\infty} nW_A(n)}{\sum_{n=1}^{\infty} nW_A(n)} \quad (5a)$$

$$\delta_B(n_B^*, x_B) = \frac{\sum_{n=n_B^*}^{\infty} nW_B(n)}{\sum_{n=1}^{\infty} nW_B(n)} \quad (5b)$$

The same formalism could be used for analysis of transition optical rotary changes of the  $\kappa/\iota$ -hybrids,  $\Delta_t[\alpha]$ , as a function of their composition. In this case, similarly to 4 we can get that

$$\Delta_t[\alpha] = \Delta_t[\alpha]_A \delta_A(1 - x_B) + \Delta_t[\alpha]_B \delta_B x_B \quad (6)$$

where  $\Delta_t[\alpha]_A$  and  $\Delta_t[\alpha]_B$  are transition optical rotary increments of  $\iota$ - and  $\kappa$ -sequences; and the parameters  $\delta_A$  and  $\delta_B$  are defined by Eqs. 5.

## 6. Conclusions

We successfully characterised a large series of possible  $\kappa/\iota$ -hybrid carrageenans from a wide variety of botanical sources. Although the  $\kappa/\iota$ -hybrid nature has not been established by KCl fractionation, the composition dependence of the total transition enthalpy of the  $\kappa/\iota$ -hybrids is satisfactory evidence of the hybrid nature of this series of samples. Different red algae species produce  $\kappa/\iota$ -hybrids with specific ratios of  $\kappa$ -units and  $\iota$ -units independent of seasonal variation. Pyruvate substitution was frequently observed in samples with a high  $\iota$ -content. Traces or small amounts of floridean starch were found in several samples independent of the composition.

A selected set of purified  $\kappa/\iota$ -hybrid carrageenans ranging from almost homopolymeric  $\kappa$ -carrageenan to almost homopolymeric  $\iota$ -carrageenan was used for further analysis. The physical properties of these  $\kappa/\iota$ -hybrids differ considerably from those of simple mixtures of homopolymeric  $\kappa$ - and  $\iota$ -carrageenan. The highest gel strength, expressed in terms of the storage modulus ( $G'$ ), was observed for homopolymeric  $\kappa$ -carrageenan. With decreasing  $\kappa$ -content the gel strength of the  $\kappa/\iota$ -hybrids decreases. On the other hand, the gelation temperature of the  $\kappa$ -rich  $\kappa/\iota$ -hybrids, defined as the crossover point of the storage and loss moduli ( $G' = G''$ ) is independent of their composition. This allows the gel strength to be controlled independent of the gelation or melting temperature.

In respect of ordering capability,  $\iota/\kappa$ -hybrid carrageenans seem to behave as AB random block copolymers with length sequence distributions truncated from a side of small lengths. Intrinsic thermodynamic properties of AA and BB sequences in these copolymers are close to those of their parent homopolymers. The truncating limit for  $\kappa$ -sequences is 2-fold larger than that for  $\iota$ -sequences. It seems to be caused by a difference in the nucleation constants for  $\kappa$ - and  $\iota$ -double helices. The truncating limit for  $\iota$ -sequences in  $\nu$ -carrageenans is much larger than that in the  $\kappa/\iota$ -hybrids.

## Acknowledgements

The authors gratefully acknowledge Dr. Georg Therkelsen (CP Kelco, Lille Skensved, Denmark) for helpful discussions and critically reading the manuscript and for performing the rheological measurements. A.S.A. thanks the graduated school VLAG (Advanced Studies in Food Technology, Agrobiotechnology, Nutrition and Health Sciences) for financial support. V.Ya.G, T.V.B. and N.V.G. thank the Netherlands Organisation for Scientific Research (NWO, the Netherlands, Project 047.009.016) for partial financial support.

## References

1. Van de Velde, F.; Peppelman, H. A.; Rollema, H. S.; Tromp, R. H. *Carbohydr. Res.* **2001**, *331*, 271–283.
2. Van de Velde, F.; De Ruiter, G. A. In *Polysaccharides II: Polysaccharides from Eukaryotes*; Steinbüchel, A., DeBaets, S., VanDamme, E. J., Eds.; Biopolymers; Wiley-VCH: Weinheim, 2002; Vol. 6, pp 245–274.
3. Therkelsen, G. H. In *Industrial Gums: Polysaccharides and their Derivatives*; Whistler, R. L., BeMiller, J. N., Eds.; Academic: San Diego, 1993; pp 145–180.
4. Imeson, A. P. In *Handbook of Hydrocolloids*; Phillips, G. O., Williams, P. A., Eds.; Woodhead Publishing: Cambridge, 2000; pp 87–102.
5. Knutsen, S. H.; Myslabodski, D. E.; Larsen, B.; Usov, A. I. *Bot. Mar.* **1994**, *37*, 163–169.
6. Rudolph, B. In *Marine and Freshwater Products Handbook*; Martin, R. E., Carter, E. P., Davis, L. M., Flich, G. J., Eds.; Technomic Publishing Company: Lancaster, USA, 2000; pp 515–529.
7. McCandless, E. L.; West, J. A.; Guiry, M. D. *Biochem. Syst. Ecol.* **1982**, *10*, 275–284.
8. Falshaw, R.; Bixler, H. J.; Johndro, K. *Food Hydrocolloids* **2003**, *17*, 129–139.
9. Rochas, C.; Rinaudo, M.; Landry, S. *Carbohydr. Polym.* **1989**, *10*, 115–127.
10. Bixler, H. J.; Johndro, K.; Falshaw, R. *Food Hydrocolloids* **2001**, *15*, 619–630.
11. Falshaw, R.; Bixler, H. J.; Johndro, K. *Food Hydrocolloids* **2001**, *15*, 441–452.
12. Villanueva, R. D.; Mendoza, W. G.; Rodriguez, M. R. C.; Romero, J. B.; Montano, M. N. E. *Food Hydrocolloids* **2004**, *18*, 283–292.
13. Bixler, H. J. *Hydrobiologia* **1996**, *326/327*, 35–57.

14. Chopin, T.; Sharp, G.; Belyea, E.; Semple, R.; Jones, D. *Hydrobiologia* **1999**, 398/399, 417–425.
15. Santelices, B. *Hydrobiologia* **1999**, 398/399, 15–23.
16. Amimi, A.; Mouradi, A.; Givernaud, T.; Chiadmi, N.; Lahaye, M. *Carbohydr. Res.* **2001**, 333, 271–279.
17. Falshaw, R.; Furneaux, R. *Carbohydr. Res.* **1994**, 252, 171–182.
18. Falshaw, R.; Furneaux, R. H. *Carbohydr. Res.* **1995**, 276, 155–165.
19. Estevez, J. M.; Ciancia, M.; Cerezo, A. S. *J. Phycol.* **2002**, 38, 344–350.
20. Ciancia, M.; Matulewicz, M. C.; Finch, P.; Cerezo, A. S. *Carbohydr. Res.* **1993**, 238, 241–248.
21. Miller, I. J. *Bot. Mar.* **2003**, 46, 572–577.
22. Stortz, C. A.; Bacon, C. E.; Cherniak, R.; Cerezo, A. S. *Carbohydr. Res.* **1994**, 261, 317–326.
23. Pereira, L.; Sousa, A.; Coelho, H.; Amado, A. M.; Ribeiro-Claro, P. J. A. *Biomol. Eng.* **2003**, 20, 223–228.
24. Pereira, L.; Mesquita, J. F. *Biomol. Eng.* **2003**, 20, 217–222.
25. Van de Velde, F.; Knutsen, S. H.; Usov, A. I.; Rollema, H. S.; Cerezo, A. S. *Trends Food Sci. Technol.* **2002**, 13, 73–92.
26. Van de Velde, F.; Rollema, H. S.; Grinberg, N. V.; Burova, T. V.; Grinberg, V. Y.; Tromp, R. H. *Biopolymers* **2002**, 65, 299–312.
27. Van de Velde, F.; Pereira, L.; Rollema, H. S. *Carbohydr. Res.* **2004**, 339, 2309–2313.
28. Chiovitti, A.; Bacic, A.; Craik, D. J.; Kraft, G. T.; Liao, M.-L.; Falshaw, R.; Furneaux, R. H. *Carbohydr. Res.* **1998**, 310, 77–83.
29. Piculell, L. In *Food Polysaccharides and their Applications*; Stephan, A. M., Ed.; Marcel Dekker: New York, 1995; pp 205–244.
30. Nilsson, S.; Piculell, L. *Macromolecules* **1989**, 22, 3011–3017.
31. Viebke, C.; Piculell, L.; Nilsson, S. *Macromolecules*, **1994**, 27, 4160–4166.
32. Applequist, J. In *Conformation of Biopolymers*; Ramachandran, G. N., Ed.; Academic: New York, 1967; pp 403–425.
33. Rochas, C.; Rinaudo, M.; Vincendon, M. *Int. J. Biol. Macromol.* **1983**, 5, 111–115.
34. Chen, Y.; Liao, M.-L.; Dunstan, D. E. *Carbohydr. Polym.* **2002**, 50, 109–116.
35. Ridout, M. J.; Garza, S.; Brownsey, G. J.; Morris, V. J. *Int. J. Biol. Macromol.* **1996**, 18, 5–8.
36. Deneff, B.; Mischenko, N.; Koch, M. H. J.; Reynaers, H. *Int. J. Biol. Macromol.* **1996**, 18, 151–159.
37. Bongaerts, K.; Reynaers, H.; Zanetti, F.; Paoletti, S. *Macromolecules* **1999**, 32, 675–682.
38. Bongaerts, K.; Paoletti, S.; Deneff, B.; Vanneste, K.; Cuppo, F.; Reynaers, H. *Macromolecules* **2000**, 33, 8709–8719.
39. Millane, R. P.; Chandrasekaran, R.; Arnott, S.; Dea, I. C. M. *Carbohydr. Res.* **1988**, 182, 1–17.
40. Cairns, P.; Atkins, E. D. T.; Miles, M. J.; Morris, V. J. *Int. J. Biol. Macromol.* **1991**, 13, 65–68.
41. Janaswamy, S.; Chandrasekaran, R. *Carbohydr. Res.* **2001**, 335, 184–194.
42. Morris, E. R.; Rees, D. A.; Robinson, G. J. *Mol. Biol.* **1980**, 138, 349–362.
43. Rees, D. A.; Williamson, F. B.; Frangou, S. A.; Morris, E. R. *Eur. J. Biochem.* **1982**, 122, 71–79.
44. Grinberg, V. Y.; Grinberg, N. V.; Usov, A. I.; Shusharina, N. P.; Khokhlov, A. R.; Kruif, K. G. d. *Biomacromolecules* **2001**, 2, 864–873.
45. Cantor, C. R.; Schimmel, P. R. *Biophysical Chemistry*; Mir: Moscow, 1985; pp 193–196.
46. Lawson, C. J.; Rees, D. A. *Nature* **1970**, 227, 392–393.
47. Vasnev, V. A.; Kutchanov, S. I. In *Polymer Encyclopedia*; Soviet Encyclopedia: Moscow, 1977; Vol. 3, pp 439–446.